D. ZHANG[1]
P. WANG[1,✉]
X. JIAO[1]
G. YUAN[1]
J. ZHANG[1]
C. CHEN[1]
H. MING[1]
R. RAO[2]

Investigation of the sensitivity of H-shaped nano-grating surface plasmon resonance biosensors using rigorous coupled wave analysis

[1] Department of Physics, University of Science and Technology of China, Hefei 230026, P.R. China
[2] Key Laboratory of Atmosphere Optics of Anhui Institute of Optics and Fine Mechanics,
    Chinese Academy of Sciences, Hefei 230031, P.R. China

ABSTRACT The sensitivity of an angle-resolved surface plasmon resonance biosensor is not only determined by the shift of the resonance angle, but also the width of the SPR curves and reflective amplitude. The three factors should be considered simultaneously in designing a SPR biosensor. In this study, a H-shaped nano-grating-based SPR biosensor is proposed and the influence of different structural parameters on the performance is investigated by using rigorous coupled wave analysis (RCWA). Electric field distribution around the nano-grating are also given out to directly explain the performance difference for various structural parameters. Larger resonance angle shift, reflectance amplitude and sharper SPR curves' width are obtained simultaneously under optimized structural parameters. Our study is usefully for understanding of the enhancement mechanism of the nano-grating SPR biosensor and also provides instructions for fabricating highly sensitive SPR biosensors.

PACS 42.79.Dj; 42.81.Gs; 73.20.Mf; 07.07.Df

1 Introduction

Surface plasmons (SPs) are waves that propagate along the surface of a conductor, usually a metal. These are essentially light waves that are trapped on the surface because of their interaction with the free electrons of the conductor. The resonant interaction between the surface charge oscillation and the electromagnetic field of the light constitutes the SPs and gives rise to its unique properties [1]. The resonance condition is very sensitive to refractive index change of the surrounding medium around the metallic thin films. So surface plasmon resonance (SPR) effect has been widely used for its attractive characteristics in optical sensor for surface chemistry and biological detection [2]. The attenuated total internal reflection method has been widely used to excite surface plasmons in conventional SPR sensors, such as Kretschmann configuration. This kind of sensor is extremely simple in structure and has been commercially available. However, its sensitivity is not high enough for some applications, such as sensing of aerosol or gas-phase release of toxins. Known to all, the use of nobel metal nano-structures allows strong optical coup-

ling of incidence light into resonances, so-called localized surface plasmons (LSPs), which are collective electrons oscillating in the metallic nano-structures. Various interactions between LSPs, SPs, and the samples on the nano-structures can lead to different properties with additional shift of resonance angle [3, 4]. And for an angle resolved biosensor, resonance angle shift, reflectance amplitude and SPR curves' width should be considered simultaneously in designing a highly sensitive SPR biosensor, and only the enhancement of resonance angle shift can not be used to describe the sensitivity enhancement of SPR biosensor comprehensively [5]. A better SPR sensor should have a larger shift of resonance angle, sharper SPR curve and larger reflectance amplitude.

2 Simulation method and model

In this study, an H-shaped nano-grating SPR biosensor shown in Fig. 1 is proposed and theoretically investigated using well established rigorous coupled wave analysis (RCWA) [6–8]. The H-shaped nano-grating is represented as a two one-dimensional array of gold wires oriented along the Y-axis with one thin gold film (thickness d_2) between them and w_1, d_1, w_2, d_3 represent the height and width of these wires. p is defined as the period of the nano-grating and the filling factors are $f_1(w_1/p)$ and $f_2(w_2/p)$. In this paper we only investigate the case of $f_1 = f_2 = f$. The H-shaped nano-grating are placed on top of a thin gold film with thickness d_4, on which SPs are excited. An attachment layer of chromium with 2 nm thickness is placed between the thin gold film and BK7 glass prism for good contact between these two layers. The antibody–analyte binding is modeled with a 1 nm thick self-assembled monolayer (SAM) that is supported by the H-shaped nano-grating. The complex indices of refraction of BK7 glass prism substrate, sample and layers of gold and chromium are the same as that of [5]. A TM-polarized monochromatic plane wave at fixed wavelength $\lambda = 633$ nm is used in our model and the incidence angle θ is scanned with an angular resolution of 0.01° as shown in Fig. 1.

Because of the coupling between the modes on opposite sides of the nano-grating, the light on the illuminated side is tunneling through a metallic slab to the exit side, on which the samples are placed. A significant feature of this structure is that most of the light transmitted is not only on the locations of the holes but also on the metal surfaces [9]. We are particularly
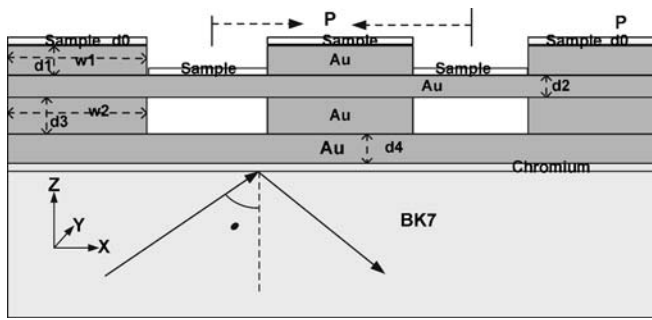
✉ Fax:+86-551-3603504, E-mail: wangpei@ustc.edu.cn

FIGURE 1   Schematic diagram of the H-shaped nano-grating SPR biosensor

interested in the influence of structural parameters on shift of resonance angle as well as width and reflectance amplitude of the SPR curves to look for balance between these three factors and, thus, optimize performance of SPR biosensor.

3   Results and discussions

Figure 2 shows the SPR curves of the H-shaped nano-grating biosensor and conventional SPR biosensor. For the conventional SPR biosensor the resonance angle shift is 0.17°, and that for the H-shaped nano-grating-based biosensor is 1.19°. In our paper the resonance angle shift sensitivity enhancement factor (RAS-SEF) is defined as the SEF of [5].

$$\text{RAS-SEF} = \frac{\theta_{\text{NWSPR}}\,(\text{sample}) - \theta_{\text{NWSPR}}\,(\text{no sample})}{\theta_{\text{SPR}}\,(\text{sample}) - \theta_{\text{SPR}}\,(\text{no sample})} \; . \quad (1)$$

In Fig. 2 the RAS-SEF is calculated to be 7 and the width of the SPR curves is also broadened at the same time. The SPR curves' width of the H-shaped nano-grating biosensor are about the same as inverses T-profile nanowire given in Fig. 2 of [5], but with a larger RAS-SEF. For SPR curve with larger width and smaller reflectance amplitude, it is more difficult to find the resonance angle, so it is necessary to obtained a sharper curves under the condition of larger RAS-SEF and
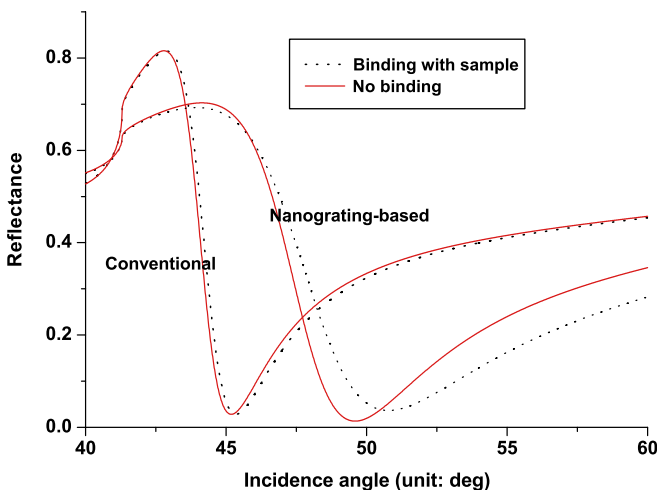
larger amplitude. In the following paragraph, the effect of the structural parameters on the performance of the H-shaped nano-grating biosensor is discussed.

3.1   *Effect of period on the sensitivity of the SPR biosensor*

In this section, influence of the nano-gratings' period is investigated. The period varies from 40 nm to 400 nm with d_1, d_2, d_3, d_4, f fixed at 15 nm, 10 nm, 10 nm, 23 nm, 0.8, respectively. The plot of RAS-SEF vs. period and SPR curves for different period are shown in Fig. 3. The calculated results shown RAS-SEF, the width and reflective amplitude of SPR curves decrease as the period enlarges. The highest RAS-SEF is 30.29 with period at 40 nm and the lowest one is 1.647 at 400 nm. To clearly show the effect of period on the performance of biosensor, the electric field distribution around the H-shaped nano-grating is given as shown in Figs. 4 and 5. Our simulated electric field distribution graph results show that electric intensity around the nano-grating decrease
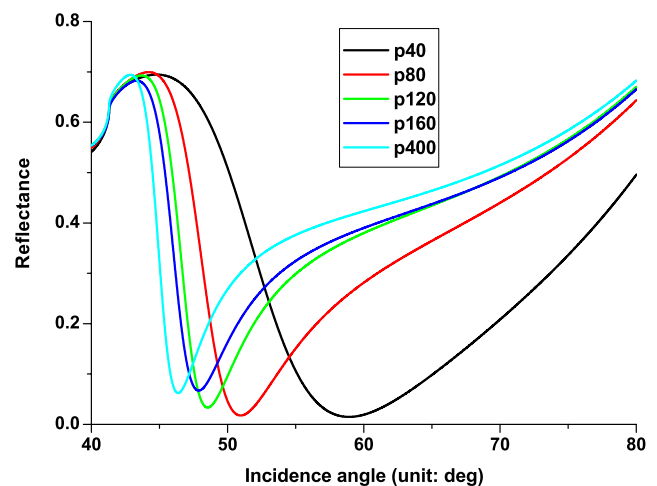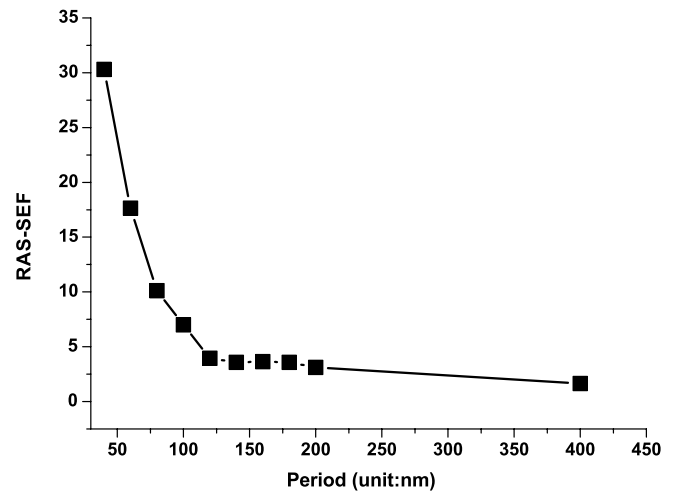

FIGURE 2   SPR curves of H-shaped nano-grating biosensor and conventional SPR biosensor. For the conventional biosensor, $d_1 = d_2 = d_3 = 0$ nm, $d_4 = 40$ nm, and the substrate is made of BK7 glass. For the H-shaped nano-grating biosensor, the structure parameters are $d_1 = 15$ nm, $d_2 = 10$ nm, $d_3 = 10$ nm, $d_4 = 23$ nm, $f = 0.8$ and $p = 100$ nm

FIGURE 3   The plot of RAS-SEF vs. period (*top*) and SPR curves for different periods (*bottom*). The values of the period varied from 40 nm to 400 nm and d_1, d_2, d_3, d_4, f are fixed at 15 nm, 10 nm, 10 nm, 23 nm, 0.8 respectively
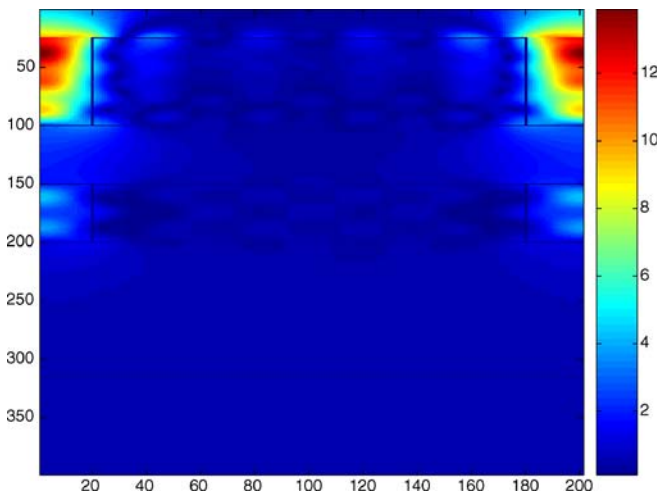
FIGURE 4 Electric field distribution around the H-shaped nano-grating ($p = 40$ nm) excited at the resonance angle – 58.92°, and we only give out the electric field distribution in one period
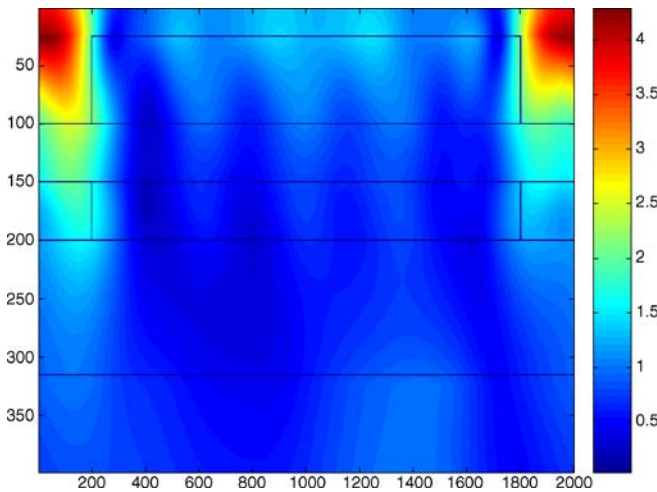

FIGURE 5 Electric field distribution of the H-shaped nano-grating ($p = 400$ nm) excited at the resonance angle – 46.38° (top), and we only provide the electric field distribution in one period

with period increasing. We only provide the distribution at 40 nm and 400 nm period, but the distribution at other period, not shown here, also confirms this trend. The reason for this trend is that stronger SPR enhancement happens at a smaller nano-grating period in this range. As a result, the stronger SPR enhancement cause larger resonant angle shift as shown in Fig. 3. The electric distribution in Figs. 4 and 5 also shown that for 40 nm period, optical intensity in the d_1 and d_3 metallic films are much larger than that for 400 nm period, which will cause more energy damping in metallic grating and result in a larger width of SPR curves, which are also consistent as the results shown in Fig. 3. So the performance difference for a different period can be explained from the electric field distribution around the nano-grating.

Although the RAS-SEF at 40 nm is very high, the SPR curves' width is so much larger that it is difficult to find the resonance angle and decrease the contrast in practice experiment. On the other hand, although the SPR curve is narrow with period at 400 nm, the RAS-SEF and reflectance amplitude is not good and the reflectance amplitude is smaller, so

a balance of these three factors should be selected. In this paper, the period at 80 nm is selected for the following investigations for its relative narrower curves width, larger RAS-SEF and reflectance amplitude.

3.2   *Effect of the filling factor on the sensitivity of the SPR biosensor*

Sensitivity of the H-shaped nano-gratings biosensor with period 80 nm and filling factor ($f = f_1 = f_2$) varying from 0.1 to 0.9 are investigated in this section. The values of d_1, d_2, d_3 are fixed at 15 nm, 10 nm and 10 nm, respectively. The calculated curves are given out in Fig. 6, which shown that the change of RAS-SEF, curves' width, and reflectance amplitude vs. filling factors is not monotonic. The performance difference for different filling factors is due to the interaction between adjacent nano-wires. The highest RAS-SEF is 14.47 with a filling factor at 0.9. Under this condition, the nano-wires are very close to each other and stronger SPR enhancement is produced, which result in larger RAS-SEF. It is worth noticing that the RAS-SEF, width and reflectance am-
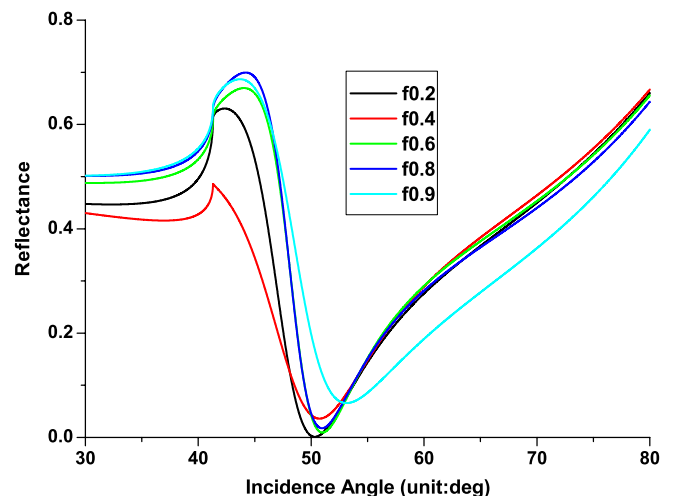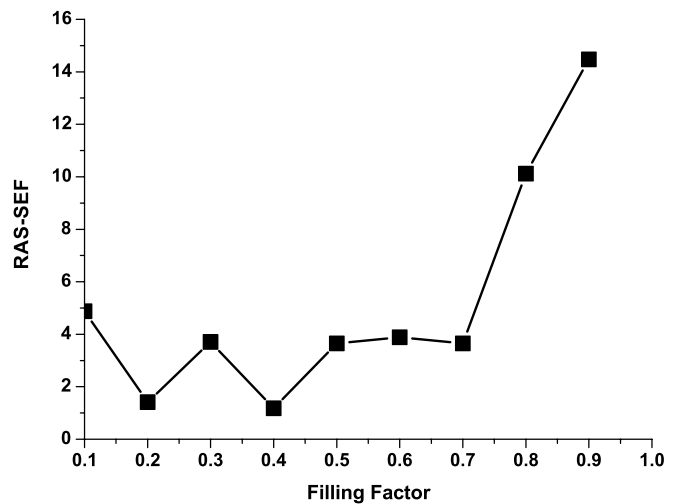

FIGURE 6 The plot of RAS-SEF vs. filling factors (*top*) and SPR curves for different filling factors (*bottom*)

plitude of curves are not good at some filling factors, such as 0.4 in this case. So in the process of fabricating nano-grating biosensor, it is necessary to avoid this instance. Although the RAS-SEF at $f = 0.9$ is larger than that at $f = 0.8$, the width and amplitude of SPR curves at $f = 0.9$ is worse than that at $f = 0.8$. So in designing of SPR biosensor, $f = 0.8$ is preferred with other parameters fixed.

3.3   *Effect of d_2 on the sensitivity of the SPR biosensor*

In the structure of the H-shaped nano-grating SPR biosensors, the thin gold film between the two one-dimensional nano-gratings plays the role of transporter of the light on the illuminated side to the upper side [10, 11]. In this paragraph, we investigate the influence of this gold film (thickness d_2) on the sensitivity of the biosensor. The values of d_1, d_3, d_4, f are fixed at 15 nm, 10 nm, 23 nm, 0.8, respectively, and d_2 varies from 0 nm to 15 nm. The calculated results are given out in Fig. 7. The curves' width and
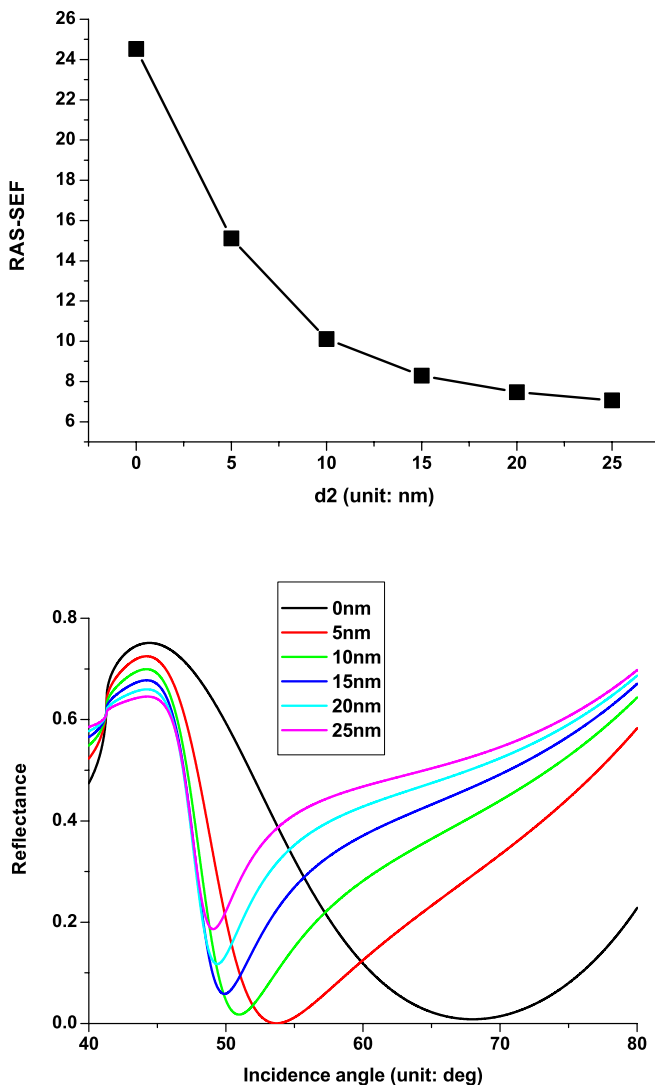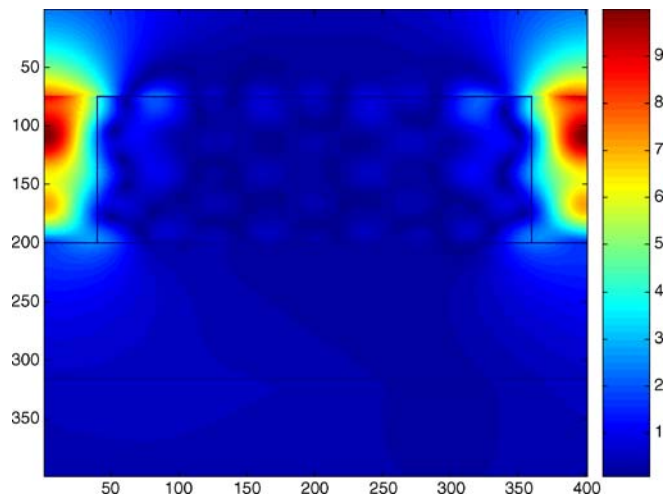

FIGURE 8   Electric field distribution of the nano-grating with $d_2 = 0$ nm excited at resonance angle – 68° and we only give out the electric field distribution in one period

RAS-SEF enhance, but the reflectance amplitude decrease as d_2 value increasing. Although the RAS-SEF with $d_2 = 0$ nm is largest, the width of the SPR curves is too large to exactly find the resonance angle.

To clearly show the role of d_2 film in this kind biosensor, electric field distribution around the nano-grating are shown in Figs. 8 and 9 for $d_2 = 0$ nm and $d_2 = 10$ nm under resonance conditions. From Fig. 9, we find that the electric field on the illuminated side is amplified by the d_2 metallic film and become larger at the exit side under both resonance condition and also non-resonance condition (the electric field distribution graph is not shown in this paper). From Fig. 9, we find that there is little energy concentrating in the d_2 film, which reduces the energy damping in the metallic film and result in narrower SPR curves.

When comparing Figs. 8 and 9, we find that optical intensity concentrated in the metallic film in the case of $d_2 = 0$ nm is larger than that in the case of $d_2 = 10$ nm under both the resonance condition and non-resonance condition according
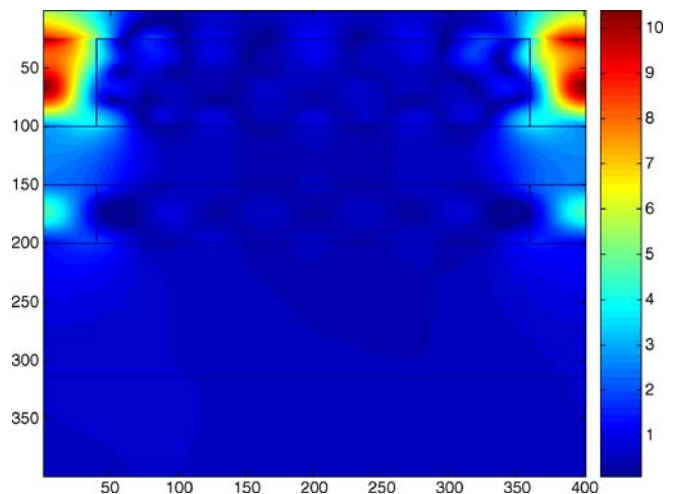

FIGURE 7   The plot of RAS-SEF vs. d_2 (*top*) and SPR curves for different d_2 values (*bottom*), The values of d_1, d_3, d_4, f are fixed at 15 nm, 10 nm, 23 nm, 0.8 respectively and d_2 varies from 0 nm to 15 nm

FIGURE 9   Electric field distribution in one period of the nano-grating with $d_2 = 10$ nm excited at resonance angle – 50.97°

to our simulation results (the electric filed distribution graphs under non-resonant conditions are not shown in this paper). So we can conclude that the optical absorption by metallic films with $d_2 = 0$ nm is much larger than that with $d_2 = 10$ nm in wide range of incidence angle, although the total thickness of metallic films used in the case of $d_2 = 0$ nm is less than that in $d_2 = 10$ nm. As a result, the SPR curves' width with $d_2 = 10$ nm is narrower than that with $d_2 = 0$ nm [12]. On the other hand, the electric field intensity with $d_2 = 0$ nm is larger under a wide range of incidence angle, so its resonance angle is more sensitive to the change of surrounding medium as shown in Fig. 7. When comparing the SPR curve for $p = 40$ nm shown in Fig. 3 and $d_2 = 10$ nm shown in Fig. 7, we find the curve's width for $p = 40$ nm is smaller than that for $d_2 = 0$ nm but with a larger RAS-SEF. This phenomenon also confirms that the existence of d_2 film can reduce the energy damping and result in narrow SPR curves.

According to our simulated results, we find the electric field intensity on the exit side will be reduced with a too large d_2 value, because for thicker metallic films, such as 15 nm or 20 nm, the light cannot pass them easily and much of the light is reflected, which results in larger reflectance at the resonance angle as shown in Fig. 7. So in the process of fabricating a biosensor, the proper d_2 value should be selected to obtain larger RAS-SEF with sharper curves and larger reflectance amplitude.

4   Summary

In summary, we have investigated the influence of the structural parameters on the sensitivity enhancement of a new H-shaped nano-grating surface plasmon resonance biosensor using RCWA. Resonant angle shift, width and amplitude of the SPR curves are considered simultaneously to optimize the sensitivity enhancement by changing the structural parameters. According to our simulated results, the H-shaped nano-grating biosensor with $p = 80$ nm, $d_1 = 15$ nm, $d_2 = 10$ nm, $d_3 = 10$ nm, $d_4 = 23$ nm performs best when the three factor are considered. What is more, the electric field distribution around the nano-grating are given to directly explain the performance difference for different structural parameters, and this method has not been used in any other articles to our knowledge. The analysis used in this paper can also be used to analyze the performance of others SPR biosensors to find the best optimized nano-structures. Our study will be useful for understanding of sensitivity enhancement mechanism of the nano-grating biosensor and development of highly sensitive biosensor.

REFERENCES

1 W.L. Barnes, A. Dereux, T.W. Ebbesen, Nature **24**, 824 (2003)
2 J. Homola, S.S. Yee, G. Gauglitz, Sens. Actuators B **54**, 3 (1999)
3 L. He, M.D. Musick, S.R. Nicewarner, F.G. Salinas, S.J. Benkovic, M.J. Natan, C.D. Keating, J. Am. Chem. Soc. **122**, 9071 (2000)
4 A.J. Haes, R.P. Van Duyne, J. Am. Chem. Soc. **124**, 10596 (2002)
5 K.M. Byun, S.J. Kim, Opt. Express **13**, 3737 (2005)
6 M.G. Moharam, T.K. Gaylord, J. Opt. Soc. Am. **71**, 811 (1981)
7 M.G. Moharam, T.K. Gaylord, J. Opt. Soc. Am. **72**, 1385 (1982)
8 M.G. Moharam, T.K. Gaylord, J. Opt. Soc. Am. A **3**, 1780 (1986)
9 X. Luo, T. Ishihara, Opt. Express **12**, 3055 (2004)
10 X. Luo, T. Ishihara, Appl. Phys. Lett. **84**, 4780 (2004)
11 D.O.S. Melville, R.J. Blaikie, C.R. Wolf, Appl. Phys. Lett. **84**, 4403 (2004)
12 C. Sonnichsen, T. Franzl, T. Wilk, G. von Plessen, J. Feldmann, O. Wilson, P. Mulvaney, Phys. Rev. Lett. **88**, 077402 (2002)